Internal Rotation and Butterfly-like Ring Inversion in 9-*tert*-Butylanthracene

Glenn H. Penner,*,† Y.-C. Phillis Chang, Patrik Nechala, and Robert Froese

Department of Chemistry and Biochemistry, University of Guelph, Guelph, Ontario, Canada N1G 2W1

Received July 17, 1998

In the solid state 9-*tert*-butylanthracene exists in a structure where the anthracene ring is nonplanar. The dihedral angle between the two lateral benzenic rings is about 18°. In addition the *tertiary* butyl group is displaced in a direction opposite to the ring bending. Ab initio molecular orbital calculations (3-21G) agree that the isolated (gas phase) molecule exists in a nonplanar geometry and indicate that there are two mechanisms for *tert*-butyl group rotation. A high-energy (35.1 kJ/mol) rotation requires a further bending of the *tert*-butyl group. The low-energy process (4.7 kJ/mol) involves a concerted *tert*-butyl rotation and butterfly-like inversion (flapping) of the anthracene fused ring. The motion of the *tert*-butyl group in solid 9-*tert*-butylanthracene was monitored by variable temperature ^{13}C CP/MAS NMR spectroscopy and appears to follow the high-energy mechanism for *tert*-butyl rotation with an activation energy of 63.1 ± 2.7 kJ/mol. The nearly 30 kJ/mol increase over the calculated value is the result of additional intermolecular interactions in the solid state. In solution (5:2 CS_2/acetone-d_6) it was not possible to stop the *tert*-butyl group rotation even at the lowest achievable temperature (ca. 150 K). This is consistent with the low-energy mechanism, where the ring inversion is not prevented by crystal packing forces.

Introduction

The rotation of *tertiary* butyl groups within organic molecules has received a significant amount of attention over the past few decades.[1−9] In particular derivatives of *tert*-butylbenzene, **1**, have been the subjects of several studies. [5−9]

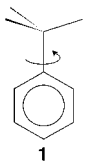

1

The internal rotational potential energy function, $V(\theta)$, for **1** and its symmetrically substituted derivatives has a 6-fold symmetry and can be written as

$$V(\theta) = V_6 \sin^2(3\theta) + V_{12} \sin^2(6\theta) \qquad (1)$$

where V_6 is the barrier height and the ratio V_6/V_{12} determines the shape of the potential energy function. In the case of derivatives of lower symmetry the potential energy function may take the form[12]

$$V(\theta) = V_3 \sin^2(^3/_2\theta) + V_6 \sin^2(3\theta) \qquad (2)$$

It is interesting that in isolated **1** the rotation of the methyl groups requires about 12 kJ/mol, whereas the *tert*-butyl group only needs to surmount a barrier of a few kJ/mol. This situation changes for solid derivatives of **1** where *inter*molecular interactions due to crystal packing forces increase the barrier for *tert*-butyl rotation and reduce the symmetry of the potential from 6-fold to 3-fold. In contrast the methyl rotational barrier, which is dominated by *intra*molecular interactions, changes very little.

Most of the earlier work on *tert*-butyl group rotation was carried out with variable temperature, dynamic NMR (DNMR) spectroscopy in solution samples.[2] More recently an electron diffraction study of *tert*-butylbenzene has appeared.[1] Although solution state work is still being carried out,[3] the emphasis has recently been directed toward solid-state NMR spectroscopy and ab initio molecular orbital calculations. Riddell and co-workers have used ^{13}C dynamic NMR (DMNR) spectroscopy and measurements of the spin−lattice relaxation time in the rotating frame ($T_{1\rho}$) to look at *tert*-butyl rotation in solid aliphatic compounds.[4] Beckman and co-workers have performed ^{1}H T_1 studies of solid *tert*-butylbenzene[5a] and several derivatives.[5,7] Rotation of the *tert*-butyl and methyl groups in solid 1,4-di-*tert*-butylbenzene and its inclusion compound with thiourea has been investigated in our laboratory by deuterium line shape and T_1 measurements.[6]

† E-mail: penner@chembio.uoguelph.ca.

(1) Campanelli, A. R.; Domenicano, A.; Hargittai, I. *J. Phys. Chem.* **1994**, *98*, 11046.

(2) Two earlier reviews include the following. (a) Kessler, H. *Angew. Chem., Int. Ed. Engl.* **1970**, *9*, 219. (b) Öki, M. *Applications of Dynamic NMR Spectroscopy to Organic Molecules*; VCH: Deerfield Beech, FL, 1985 (see Chapter 6).

(3) Port, A.; Morgas, M.; Sánches-Ruiz, X.; Jaime, C.; Virgili, A.; Alvarez-Larena, A.; Piniella, J. F. *J. Org. Chem.* **1997**, *62*, 899.

(4) (a) Riddell, F. G.; Rogerson, M. *Magn. Reson. Chem.* **1997**, *35*, 333. (b) Riddell, F. G.; Arumugam, S.; Harris, K. D. M.; Rogerson, M.; Strange, J. H. *J. Am. Chem. Soc.* **1993**, *115*, 1881. (c) Riddell, F. G.; Arumugam, S.; Anderson, J. E. *J. Chem. Soc., Chem. Commun.* **1991**, 15. (d) Riddell, F. G.; Bernath, G.; Fülöp, F. *J. Am. Chem. Soc.* **1995**, *117*, 2327.

(5) (a) Beckman, P. A.; Hathorn, R. M.; Mallory, F. B. *Mol. Phys.* **1998**, *69*, 411. (b) Fry, A. M.; Beckman, P. A.; Fry, A. J.; Fox, P. C.; Isenstadt, A. *J. Chem. Phys.* **1991**, *95*, 4778.

(6) Penner, G. H.; Polson, J. M.; Stuart, C.; Ferguson, G.; Kaitner, B. *J. Phys. Chem.* **1992**, *96*, 5121.

(7) (a) Aronson, M.; Beckman, P. A.; Ross, B.; Tan, S. L. *Chem. Phys.* **1981**, *63*, 349. (b) Beckman, P. A.; Fusco, F. A.; O'Neill, A. E. *J. Magn. Reson.* **1984**, *59*, 63. (c) Beckman, P. *Chem. Phys.* **1981**, *63*, 359.

(8) Schaefer, T. P.; Penner, G. H. *J. Mol. Struct. (THEOCHEM)* **1986**, *138*, 305.

(9) Penner, G. H.; Chang, P. Unpublished results.

10.1021/jo981402g CCC: $18.00
Published on Web 12/31/1998

Molecular orbital (MO) calculations have concentrated on *tert*-butyl rotation in derivatives of **1**, and V_6 has been calculated to be 3.0 kJ/mol using the STO-3G basis set.[8] Later calculations gave values of 2.8 kJ/mol (6-31G) and 2.9 kJ/mol (6-31G*).[1] In all cases the lowest energy conformation has one C−C bond in the phenyl ring plane. The only experimental value for the torsional barrier available for **1** as an isolated molecule in the gas phase is the result of an electron diffraction study by Hargittai and co-workers.[1] They estimate a V_6 value of 4.7 ± 2.7 kJ/mol on the basis of the average twist angle of the *tert*-butyl substituent.

An interesting and unusual derivative (loosely speaking) of **1** is 9-*tert*-butylanthracene, **2**. This molecule is of interest in that it represents a situation where the *tert*-butyl group is highly hindered by two adjacent C−H bonds, both of which point directly at the *tert*-butyl group. If a planar anthracene ring is assumed, a barrier of 44.0 kJ/mol is calculated (3-21G).[9] This is in the range where NMR and line shape analysis should be applicable. Compound **2** is unusual in that the anthracene fused ring system is, in fact, not planar in the solid state as shown by X-ray crystallography[10] (vide infra). No ab initio molecular orbital calculations on **2** have been reported. We have undertaken the synthesis of **2** and **2**-d_9 and investigate the structure and dynamics of the *tert*-butyl and methyl groups in **2** by ^{13}C DNMR in solution and by ^{13}C CP/MAS DNMR, ^{2}H line shapes, and ^{2}H spin−lattice relaxation times in the solid state. In addition the structure and internal rotation in **2** is investigated by ab initio MO calculations.

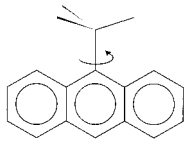

2

Experimental Section

A sample of **2** was prepared by the method of Parish and Stock[11] with the slight modification that the *tert*-butylmagnesium chloride was prepared in THF. A sample of **2**-d_9 was prepared using *tert*-butyl chloride-d_9. The identity and purity of the sample were checked by solution ^{13}C and ^{1}H NMR spectroscopy.[11b]

^{13}C CP/MAS NMR spectra were recorded on a Bruker ASX 200 spectrometer at a frequency of 50.32 MHZ. The ^{13}C $\pi/2$ pulses were 4.0 μs, and cross-polarization times of 3 ms were used. Typically 100−150 transients were accumulated, and the recycle delay was 5 s. The samples were spun at 4 kHz, using a 7 mm Bruker MAS probe. The chemical shifts were referenced to the low-frequency signal of adamantane (29.5 ppm), and following acquisition, an exponential apodization of 10 Hz was applied before the Fourier transform. The spinning sample was cooled by high-pressure nitrogen gas which was in turn cooled by passing the gas through a coil submersed in liquid nitrogen. The temperate of the bearing gas was regulated by a Eurotherm B-VT 2000 temperature controller. The temperature was calibrated by the method of Riddell et al.[12] for a spinning rate of 4 kHz. The estimated uncertainty in the sample temperature was about 2 K.

The deuterium spectra were recorded at 30.72 MHz, using the quadrupolar echo pulse sequence:[13] $(\pi/2)_x-\tau_Q-(\pi/2)_y-\tau_Q-$acquire. The length of the $\pi/2$ pulse was approximately 2.5 μs. At each temperature, the echo signals were collected for a τ_Q value of 40 μs. The echo signals were Fourier transformed to obtain the deuterium NMR spectra. The temperature of the sample chamber was electronically regulated by a Eurotherm B-VT 2000 temperature controller to within ±0.2 °C over the course of the experiment. The true temperature of the sample was recorded just prior to each measurement by lowering a copper−constantan thermocouple down the gas venting tube until it came into contact with the sample coil. The estimated uncertainty of the recorded sample temperature was about ±0.5 °C.

The deuterium T_1 data were acquired using an inversion−recovery pulse sequence modified for quadrupolar nuclei: $(\pi)_x-\tau-(\pi/2)_{\pm x}-\tau_Q-(\pi/2)_y-\tau_Q-$acquire. Typically, 12 values of τ were used to determine T_1 at each temperature. The pulse spacing, τ_Q, for the T_1 determination was 40 μs. The time between repetitions of the pulse sequence was always greater than $5T_1$. The integrated spectral intensities were fit using a nonlinear least squares algorithm employing an exponential fitting function to obtain the relevant relaxation time parameters.

Solution NMR spectra were recorded on a Varian Unity-400 NMR spectrometer. The probe temperature had been previously calibrated with methanol. The uncertainty in sample temperature was about ±2.0 K.

Quadrupolar echo spectra were simulated by standard methods using the program MXQET.[14] Simulated spectra were visually matched to experimental line shapes. The T_1 data was least-squares fit to the BPP spectral density function[15] to obtain the activation energy, E_a, the correlation time at infinite temperature, τ_∞, and the effective quadrupolar coupling constant, χ_{eff}.

Molecular orbital calculations were performed using GAUSSIAN 94[16] on a Silicon Graphics Power Series 8 computer.

Although the crystal structure of **2** is known,[10] we chose to remove a small single crystal from *our* sample of **2**-d_9 and determine the crystal and molecular structure. This was an important proceedure as molecular dynamics in solids can be critically dependent on the *crystal* structure. Riddell et al.[4d] have shown that *tert*-butyl dynamics in organic molecules can vary significantly from one solid phase to another. Since our crystal and molecular structure simply confirms that of a previous investigation,[10] we do not report the details of our X-ray analysis. All crystal structures were obtained at ambient (room) temperature.

Results and Discussion

X-ray Crystal Structure. Two views of the crystal structure of **2** are shown in Figure 1. The deviation of the anthracene ring from planarity is obvious. The mean angle between the two halves of the central ring is 13.5°. The C_{13}–C_{15} bond is bent in a direction opposite to that of the ring distortion. The C_5, C_7, C_{12}, and C_{14} carbons of the central ring form a good plane (rms deviation 0.002

(10) (a) Jahn, B.; Dreeskamp, H. *Ber. Bunsen-Ges. Phys. Chem.* **1984**, *88*, 42. (b) Angermund, K.; Goddard, R.; Krüger, C. *Acta Crystallogr.* **1984**, *A40*, C162.

(11) (a) Parish, R. C.; Stock, L. M. *J. Org. Chem.* **1966**, *31*, 4265. (b) Bullpitt, M.; Kitching, W.; Adcock, W.; Doddrell, D. *J. Organomet. Chem.* **1976**, 161.

(12) Riddell, F. G.; Spark, R. A.; Günther, G. U. *Magn. Reson. Chem.* **1996**, *34*, 824.

(13) Davis, J. H.; Jeffrey, K. R.; Bloom, M.; Valic, M. I.; Higgs, T. P. *Chem. Phys. Lett.* **1976**, *42*, 390.

(14) Greenfield, M. S.; Ronemus, A. D.; Vold, R. L.; Vold, R. R.; Ellis, P. D.; Raidy, T. R. *J. Magn. Reson.* **1987**, *72*, 89.

(15) Bloembergen, N.; Purcell, E. M.; Pound, R. V. *Phys. Rev.* **1948**, *73*, 679.

(16) Gaussian 94 (Revision a.1); Frisch, M. J.; Trucks, G. W.; Schlegel, H. B.; Gill, P. M. W.; Johnson, B. G.; Robb, M. A.; Cheeseman, J. R.; Keith, T. A.; Petersson, G. A.; Montgomery, J. A.; Raghavachari, K.; Al-Laham, M. A.; Zakrzewski, V. G.; Ortiz, J. V.; Foresman, J. B.; Cioslowski, J.; Stefano, B. B.; Nanayakkara, A.; Challacombe, M.; Peng, C. Y.; Ayala, P. Y.; Chen, W.; Wong, M. W.; Andres, J. L.; Replogle, E. S.; Gomperts, R.; Martin, R. L.; Fox, D. J.; Binkley, J. S.; Defrees, D. J.; Baker, J.; Stewart, J. P.; Head-Gordon, M.; Gonzalez, C.; Pople, J. A. Gaussian, Inc.: Pittsburgh, PA, 1995.

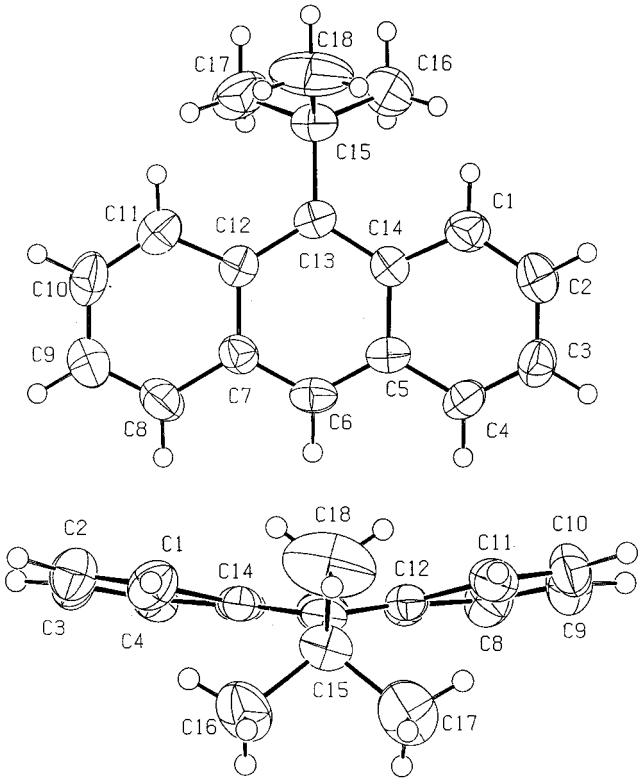

Figure 1. Two views of the molecular structure of crystalline **2** as determined by X-ray diffraction techniques.

Å). The dihedral angles $C_7-C_{12}-C_{13}-C_{15}$ and $C_5-C_{14}-C_{13}-C_{15}$ are 21.9° and 21.6°, respectively. The two side rings also form reasonably good planes (rms 0.024 and 0.034 Å, respectively), and the angle between these planes is 17.8°. In the solid state, molecular **2** belongs to the point group C_1. Therefore there is no C_2 axis or plane of symmetry. As a result, all three methyl carbons are expected to be chemically nonequivalent. The methyl groups can occupy three positions, therefore $V(\theta)$ should be 3-fold symmetric, not 6-fold as expected for a planar anthracene ring.

The deviation from planarity of the anthracene ring in **2** is not unique. Other bulky substituents such as pivaloyl[3] or trimethylsilyl[17] groups have also resulted in nonplanar ring structures.

Molecular Orbital Calculations. Table 1 provides some relevant geometric parameters for **2** optimized at the 3-21G level. These compare favorably with the solid-state values. Our investigation of the internal rotation of the *tert*-butyl group (3-21G) in **2** yielded a rather intriguing result. Upon rotation of the *tert*-butyl group by about 30°, the anthracene ring becomes planar (all ring carbon and hydrogen atoms are within 0.3° of being coplanar) and a further rotation results in an inversion of the fused rings to yield a mirror image of the original structure. This flapping of the anthracene ring resembles a butterfly-like motion. The total energy required for this concerted internal rotation/inversion process is only 4.7 kJ/mol! The *tert*-butyl group may also rotate without ring inversion via a transition state. The total energy required for this motion is 35.1 kJ/mol. A single-point calculation at the 6-311G** level using the 3-21G geometries gave

Table 1. Carbon−Carbon Dihedral Angles Illustrating the Nonplanarity of the Anthracene Rng and the Positions of the *tert*-Butyl Carbons

dihedral angle[a]	X-ray	MO
C2−C1−C14−C13	−178.4	−178.2
C3−C4−C5−C14	4.8	0.7
C1−C2−C3−C4	−4.3	−4.1
C2−C3−C4−C5	0.5	1.3
C3−C4−C5−C6	−174.8	−174.2
C5−C6−C7−C8	−171.5	−172.5
C6−C7−C8−C9	173.6	175.7
C7−C8−C9−C10	−1.3	−0.7
C8−C9−C10−C11	9.2	3.1
C9−C10−C11−C12	1.9	−0.7
C15−C13−C12−C11	26.4	23.2
C14−C13−C15−C16	30.5	18.3
C14−C13−C15−C17	−93.8	−103.6
C14−C13−C15−C18	143.3	132.0

[a] The carbons are numbered according to Figure 1.

an energy difference of 35.5 kJ/mol. A plot of the relative energies for the rotation/inversion process as a function of the angle $C_{14}-C_{13}-C_{15}-C_{16}$ is shown in Figure 3. These points can be fit to eq 3, a modification of eq 1 to yield $\theta_0 = 47.7 \pm 0.3$, $V_6 = 4.5 \pm 0.2$ kJ/mol, and $V_{12} = -0.1 \pm 0.2$ kJ/mol. A calculation of the barrier to internal

$$V(\theta) = V_6 \sin^2[3(\theta - \theta_0)] + V_{12} \sin^2[6(\theta - \theta_0)] \quad (3)$$

rotation when the anthracene ring is held planar but all other geometric parameters are allowed to relax gave $V_6 = 44.0$ kJ/mol[9] with the lowest energy structure having one of the C−C bonds in the anthracene plane. The energy of this structure is 20.0 kJ/mol higher than that when the rings are allowed to relax and deviate from planarity.

Solution ^{13}C NMR. According to the structures obtained from X-ray crystallography and ab initio MO calculations, if the rotation of the *tert*-butyl group in **2** can be stopped on the ^{13}C NMR time scale, the ^{13}C spectrum should be a 1:1:1 triplet, since the structure predicts all three methyl carbons to be chemically nonequivalent. Furthermore there could also be an observed nonequivalence of various pairs of ring carbons.

The solubility of **2** is poor in most solvents but a 5:2 mixture of CS_2/acetone-d_6 allowed us to bring a dilute solution down to about 150 K without significant precipitation or freezing of the solvent.[18] Even at 150 K there was no observable splitting or any significant line shape changes in the ^{13}C spectrum. The spectral peaks were somewhat broadened due to the increase in viscosity of the sample at lower temperatures. In contrast, for 9-isopropylanthracene,[18] where the anthracene ring bisects the isopropyl group in the lowest energy structure, the internal rotation of the isopropyl group can be frozen out (7:2 CS_2:acetone-d_6) below 250 K.

Solid State ^{13}C CP/MAS. Figure 2 shows the aliphatic region of the ^{13}C CP/MAS spectrum as a function of temperature. At the lowest temperature all three methyl carbons are chemically nonequivalent, two of the methyl resonances being quite close together. This is in agreement with the crystal structure of solid **2**. Simulations of the spectral line shapes for different rates of three-site exchange are also shown in Figure 3. These temperature-dependent rates can be fit to the Arrhenius equation to yield a preexponential factor, A, of $7.68 \pm 0.95 \times$

(17) Lehmkuhl, H.; Shakoor, A.; Mehler, K.; Krüger, C.; Angermund, K.; Tsay, Y.-H. *Chem. Ber.* **1985**, *118*, 4239.

(18) Ernst, L.; Mannschreck, A. *Chem. Ber.* **1977**, *110*, 3258.

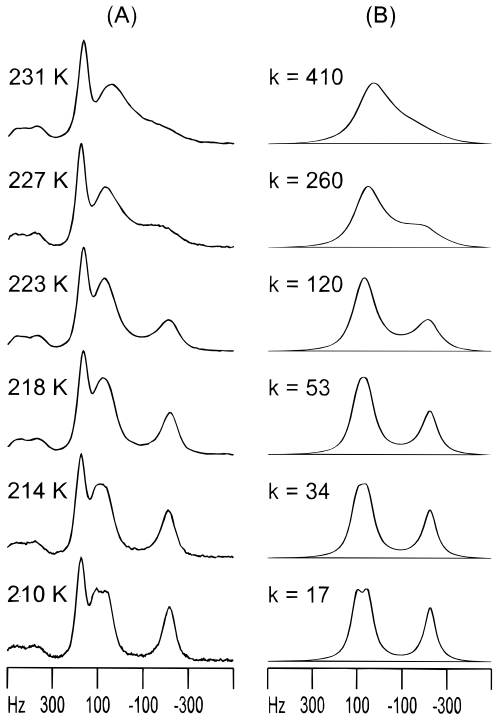

Figure 2. Carbon-13 CP/MAS spectra of **2** at various temperatures together with simulations for different rates of *tert*-butyl rotation.

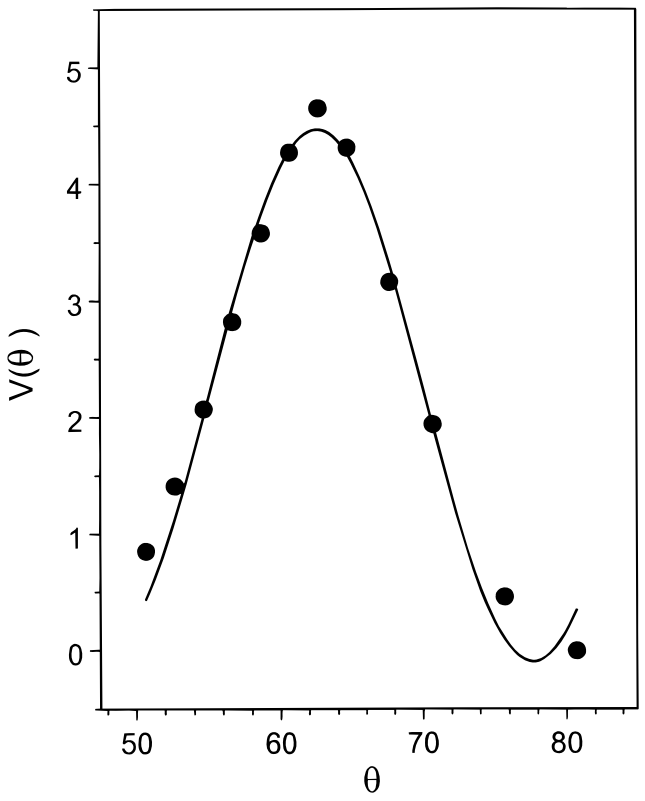

Figure 3. A plot of the calculated energy of **2** (3-21G) as a function of the torsion angle $C_{14}-C_{13}-C_{15}-C_{16}$. The solid curve is the result of a fit of the calculated points to eq 1.

10^{16} s^{-1} and an activation energy, E_a, of 63.1 ± 2.7 kJ/mol for the *tert*-butyl group rotation. The value of E_a is somewhat higher than the calculated value due to additional intermolecular interactions between the *tert*-butyl group and neighboring molecules in the crystal lattice. It should be pointed out that the ring region of the ^{13}C spectrum (not shown) changes very little as a function of temperature and is therefore rather uninformative with respect to the *tert*-butyl group dynamics.

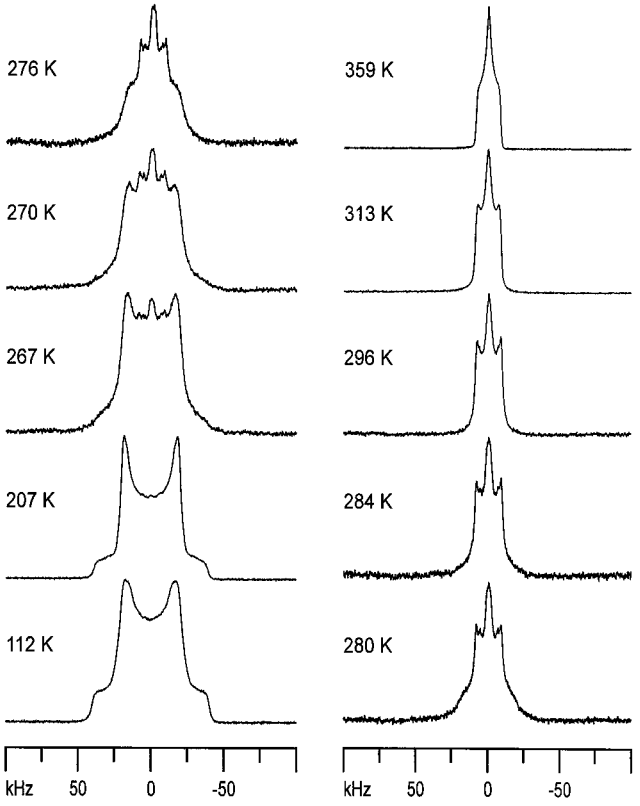

Figure 4. The deuterium NMR powder spectra of **2**-d_9 as a function of temperature.

Deuterium NMR Spectra. The deuterium powder spectra of solid **2**-d_9, at different temperatures, are shown in Figure 4. The change in line shape reflects the change in the dynamics of the *tert*-butyl hydrogens with temperature. One can begin the analysis of these spectra with the assumption that there are two motions affecting the ^2H line shape, methyl rotation and *tert*-butyl rotation. If both motions are slow on the ^2H NMR time scale ($k,k' < 10^3$ s^{-1}), a typical "Pake" powder spectrum is observed, consisting of symmetrically spaced "horns" and shoulders. The spacing between the horns, referred to as the quadrupolar splitting, is $^3/_4$ the quadrupolar coupling constant, χ. The separation between the shoulders is twice this value. The χ value obtained from the lowest temperature (112 K) spectrum is 60 ± 2 kHz. This is much too low for a typical aliphatic $C-^2H$ deuteron (170 ± 10 kHz). A more reasonable model is that of rapid methyl rotation ($k' > 10^7$ s^{-1}) and slow *tert*-butyl rotation ($k < 10^3$ s^{-1}). In that case the width of the powder spectrum is compressed (averaged) by a factor of $^1/_2(3\cos^2\theta' - 1)$, where θ' is the angle between the methyl rotational axes (C−C bonds) and the $C-^2H$ bonds. If a tetrahedral geometry is assumed, the reduction factor is $^1/_3$. This means that the unaveraged quadrupolar coupling constant is 180 ± 6 kHz. This is in the expected range of 170 ± 10 kHz. The implications are that at 112 K the methyl groups are still rotating rapidly, i.e., at rates greater than 10^7 s^{-1}. Therefore line shape changes at higher temperatures are likely due to the dynamics of

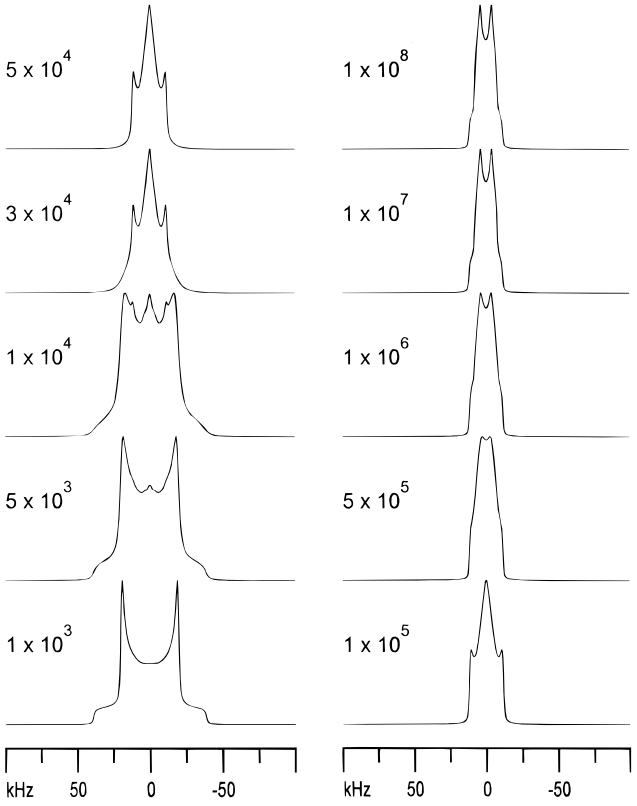

Figure 5. Simulations of the deuterium powder spectra for different rates of *tert*-butyl rotation using the X-ray *tert*-butyl group geometry.

the *tert*-butyl group. If the positions of the methyl groups are taken from the X-ray crystal structure, the ^{2}H spectra can be simulated for different rates of the *tert*-butyl group rotation that exchanges these methyl groups. These simulations are shown in Figure 5. Although the simulated and experimental spectra show many similarities at lower temperatures, the match is not satisfactory. In addition, the fast rate simulations do not fit the higher temperature spectra. Simulations employing an ideal tetrahedral *tert*-butyl group geometry show worse agreement. There are two possible explanations for the disagreement between the simulated and experimental spectral line shapes. First, as the sample temperature approaches the melting point, the molecule as a whole may begin to undergo a librational motion, the amplitude of which could increase with increasing temperature. Such a motion would produce the observed higher temperature spectra. Unfortunately simulation of these line shapes would require knowledge of the potential energy function that governs the librational motion or alternatively the distribution function for the librational angles, both of which are likely to be dependent on temperature. Another possibility is that the methyl group geometries deviate significantly from the ideal tetrahedral geometry. X-ray crystal structures do not normally provide accurate hydrogen positions. Using the *tert*-butyl structure obtained from the optimized geometry does not yield any improvement in the simulated line shapes. The ^{2}H line shape results provide a means by which to check, qualitatively, the results of the ^{13}C CP/MAS experiments. The ^{2}H line shapes should change for *tert*-butyl rotation rates of 5×10^3 up to 5×10^6 s^{-1}. Below and above these rates the line shapes do not change with changing rates.

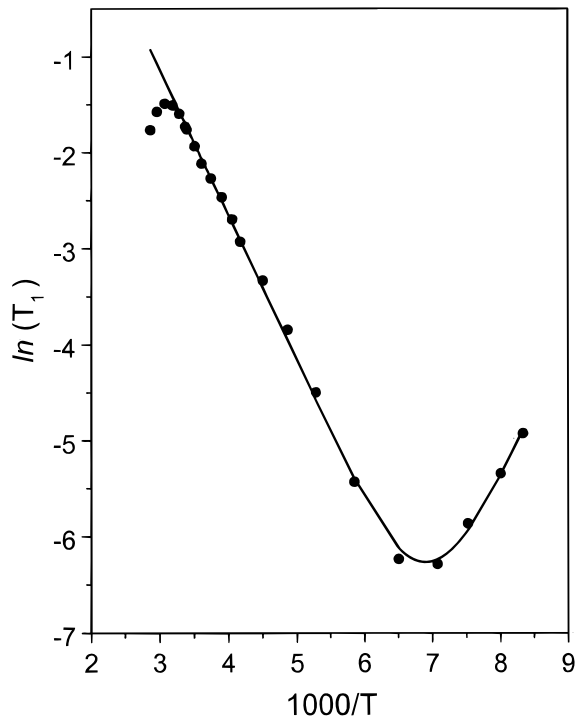

Figure 6. Deuterium spin−lattice relaxation times (T_1) as a function of inverse temperature for **2**-d_9. The solid line is a fit of the low-temperature experimental points to eqs 3 and 4.

Using E_a and A from the ^{13}C line shape analysis predicts that the ^{2}H line shapes should change in the temperature range of 250−325 K. This is indeed the temperature range in which the ^{2}H line shape changes are observed.

Deuterium Spin−Lattice Relaxation Times, T_1. The ^{2}H T_1 curve over the temperature range of 110−360 K (10° below the melting point) is presented in Figure 6. The T_1 passes through a minimum of 1.9 ms at about 145 K. The T_1 minimum corresponds to the optimum rate of C−^{2}H bond reorientation for the stimulation of spin−lattice relaxation of the ^{2}H nucleus. The T_1 curve can be fit to the BPP[14] equation (eq 4)

$$\frac{1}{T_1} = K\left(\frac{\tau_c}{1+\omega_0^2\,\tau_c^2} + \frac{4\tau_c}{1+4\omega_0^2\,\tau_c^2}\right) \qquad (4)$$

which relates the T_1 to the correlation time, τ_c, for the relavent motion. For an n-site jumping motion, the correlation time can be related to the rate by $\tau_c = 1/(nk')$. The constant K is dependent on the angle of the C−^{2}H bond with respect to the axis or axes of rotation and on the magnitude of χ. If the reorientation of the C−^{2}H bond is a thermally activated process, the τ_c dependence on temperature is given by the Arrhenius-like equation

$$\tau_c = \tau_\infty \exp\left(\frac{E_a}{RT}\right) \qquad (5)$$

where τ_c is the correlation time at infinite temperature. A fit of the experimental points around the T_1 minimum yields values of $K = 7.09 \pm 0.00 \times 10^{10}$ s^{-2}, $E_a = 12.6 \pm 0.0$ kJ/mol, and $\tau_\infty = 9.3 \pm 0.0 \times 10^{-14}$ s.

If the geometry about the methyl carbons is assumed to be tetrahedral (as it was in the last section), K is related to χ by

$$K = \frac{3\pi^2\chi^2}{10} \quad (6)$$

Solving this equation for χ yields a value of 155 ± 20 kHz, which is in reasonable agreement with the unaveraged value obtained from ^{2}H line shapes.

The activation energy of 12.6 kJ/mol is consistent with a value of 12.0 ± 0.5 for methyl rotation in the di-*tert*-butylbenzene/thiourea inclusion compound.[9] The restricted rotation of methyl groups within *tert*-butyl groups is likely to be dominated by *intra*molecular interactions within the *tert*-butyl group. One exception is 2,6-di-*tert*-butyl-4-methylphenol (also called butylated hydroxytoluene, BHT) where one methyl of each *tert*-butyl points away from the hydroxy group resulting in the rotation of these methyls being highly hindered by interaction with the *meta* C−H bonds.[19]

At higher temperatures it can be seen that the T_1 curve deviates downward. This is the result of the ^{2}H nuclear spin relaxation being stimulated by *tert*-butyl rotational motion at higher temperatures. If it were possible to measure T_1 values at higher temperatures, a second T_1 minimum would be seen and a fit of this part of the curve to eqs 4 and 5 would yield E_a, τ_∞, and K for *tert*-butyl group rotation. Unfortunately the sample begins to melt before enough high-temperature points can be measured and even an estimation of the E_a value from the high-temperature slope of the curve is not possible.

Equations 4 and 5 can be used to calculate the rates of methyl rotation at various temperatures. If we assume that the three methyl groups are dynamically equivalent and that each performs a 3-site jumping motion, the jumping rate is given as $k' = (3\tau_c)^{-1}$. At 112 K, the lowest attainable temperature a k' value of 4.8×10^6 s^{-1} is calculated. In other words, even at this low temperature the methyl groups are jumping about 5 million times a second. At 296 K (ambient temperature) this rate increases to 2×10^{10} jumps per second. This compares to a predicted rate, based on the ^{13}C line shapes, of 5.6×10^5 s^{-1} for the *tert*-butyl rotation at the same temperature.

(19) Polson, J. M.; Fyfe, J. D. D.; Jeffrey, K. R. *J. Chem. Phys.* **1991**, *94*, 3381.

Conclusions

9-*tert*-Butylanthracene, **2**, exists in a structure whereby the anthracene ring deviates significantly from planarity. This is shown to be the case for **2** in the solid state by X-ray crystallography and in the gas phase (isolated molecule) by ab initio molecular orbital calculations. Our MO calculations indicate that the rotation of the *tert*-butyl group can occur via two mechanisms. In the gas phase and in solution a mechanism involving a combined rotation of the *tert*-butyl group and butterfly-like inversion of the anthracene ring appears to take place. This process is calculated to have an unusually low activation energy of 4.7 kJ/mol. On the other hand, crystal packing forces do not allow for ring inversion in the solid state. In this case a higher energy mechanism, possibly involving the calculated transition state, is followed. We measure an activation energy of 63.1 kJ/mol for this motion by variable temperature ^{13}C CP/MAS NMR spectroscopy.

Acknowledgment. We would like to thank the Natural Sciences and Engineering Research Council (NSERC) of Canada for funding. We would also like to thank Prof. George Ferguson and Prof. John D. Goddard for help with the X-ray analysis and preliminary molecular orbital calculations, respectively.

Supporting Information Available: Tables of *z*-matrices (16 pages) for each optimized structure of **2**. See any current masthead page for ordering and Internet access instructions.

JO981402G